Cavity length downstream of a sudden fall-expansion aerator in chute

Shuai Li, Jianmin Zhang, Xiaoqing Chen, Jiangang Chen and Gordon G. D. Zhou

ABSTRACT

Cavity length has been proven to have a significant effect on the air entrainment of an aerator in flood discharge engineering; however, the estimation of both the bottom and lateral cavity lengths downstream of a sudden fall-expansion aerator remain unclear. This research conducts a series of experiments involving various approach-flow conditions and geometric parameters of an aerator. An improved solution of the cavity length for the bottom and lateral cavities is established. The proposed equation was validated through the data of experiments and predecessor formulas, and exhibited a higher precision than other methods. Both the transverse turbulence and the axial dynamic pressure are found to be related to the formation of a lateral cavity. The present method involving the lateral cavity length was developed based on dimensional analysis and experimental test. The geometric morphology of a lateral cavity exhibits a parabolic shape, which is similar to that of the bottom cavity.

Key words | cavity length, dimensional analysis, experimental, sudden fall-expansion aerator

Shuai Li
Xiaoqing Chen
Jiangang Chen
Gordon G. D. Zhou
Key Laboratory of Mountain Hazards and Earth Surface Processes,
Chinese Academy of Sciences, and Institute of Mountain Hazards and Environment, Chinese Academy of Sciences and Ministry of Water Conservancy,
Chengdu 610041,
China

Jianmin Zhang (corresponding author)
State Key Laboratory of Hydraulics and Mountain River Engineering,
Sichuan University,
Chengdu 610065,
China
E-mail: *zhangjianmin@scu.edu.cn*

SYMBOL LIST

a_x, a_y, a_z	the acceleration along the x-direction, y-direction and z-direction
b	the width of the sudden fall-expansion aerator
C	the air concentration
C_2, C_{90}	air concentration of 2% and 90%, respectively
c_f	the coefficient of air resistance
dB, dh, ds,	the width, thickness, and length of control volume
F	the transverse force
F_a	buoyancy of the air on a nappe
F_r	Froude number
F_τ	air resistance
g	gravitational acceleration
G	gravity of control volume
h	the depth of flow
H	the flow depth
$K_{1,2}$	the coefficient
L_{c-jet}	the length of the lateral cavity length
L_{d-jet}	the length of the bottom cavity length
m	the weight of control volume
$N_{1,2}$	surface tensions
$p_{1,2}$	pressures in the x-direction
p_a, p_c	the pressures close to the free surface and internal cavity, respectively
P_N	sub-pressure beneath the cavity
R	the radius of curvature
R_e	the Reynolds number (–)
t_s	the drop height of the aerator
T	time
u_y	the lateral diffusion velocity
v	the cross-sectional mean velocity
v'	the fluctuating velocity

doi: 10.2166/ws.2018.031

v_0	the cross-sectional mean velocity at the pressure outlet
x, y, z	the horizontal, transverse and vertical coordinates of the nappe profile
α	the slopes upstream of the aerator
θ	the slope downstream of the aerator
μ	the dynamic viscosity coefficient
σ	the coefficient of surface tension
ϕ	the emergence angle of the flow jet
ρ_a, ρ_w, ρ_m	density of the air, water, and air–water mixtures

INTRODUCTION

Flow aeration by aerators is an inexpensive and effective measure to prevent cavitation erosion in hydraulic engineering (Pfister *et al.* 2011; Hager & Boes 2014). Sudden fall-expansion (vertical drop and lateral enlargement) aerators are frequently adopted in flood discharge tunnels of high-head dams. The cavity length downstream of a sudden fall-expansion aerator includes the bottom cavity length and the lateral cavity length. Cavity length is one of the most important parameters that affect the air entrainment of an aerator (Wu & Ruan 2008; Wu *et al.* 2011; Wu & Ma 2013).

Dimensional concepts complemented with semi-empirical assumptions and simplified theoretical approximations have usually been adopted to estimate the bottom cavity length downstream of a bottom aerator. Those can be divided into four categories: (i) dimensional analysis (Shi *et al.* 1983; Pan & Shao 1986; Xia & Zhang 1999; Mohaghegh & Wu 2009; Pfister & Hager 2010); (ii) projectile theory (Rutschmann & Hager 1990; Ni 1993; Chanson 1995; Yang *et al.* 1996); (iii) the infinitesimal method (Wu & Ruan 2008); and (iv) numerical simulations (Zhang *et al.* 2011; Aghebatie & Hosseini 2016). Most of the methods do not or only partially consider the effect of the exit angle, flow depth, fluctuating velocity and aeration on the bottom cavity length. In terms of the scope of application, most formulas are poor in generality and low in accuracy.

Compared to the bottom cavity, there is little research on the lateral cavity length; this may be because of the unknown mechanism of the formation of the lateral cavity. A lateral deflector built on the sidewall can increase the cavity length in sudden fall-expansion aerators (Nie *et al.* 2003). These results indicate that the slope of the outlet and the shape of the lateral deflector should be considered in the estimation of the cavity length. Liu *et al.* (2008) proposed that the lateral cavity length was influenced by both the lateral aerator and the bottom aerator. The effects of aerator conformation, the flow velocity and the fluctuating velocity on the lateral cavity were analyzed by Yue *et al.* (2009), Wang *et al.* (2013) and Liu *et al.* (2015). Additionally, some empirical equations have also been established for calculating the lateral cavity length (Yue *et al.* 2009; Liu *et al.* 2015).

Although there are several methods to estimate the cavity length of a bottom aerator or a lateral aerator, few of these methods are suitable for calculating the cavity length downstream of a sudden fall-expansion aerator. A theoretical analysis based on the projectile law and micro-element method was adopted in this study to further the knowledge of cavity length and geometric morphology along the nappe downstream of a sudden fall-expansion aerator on a spillway. The improved expressions were verified through the extensive experimental data from this study and other investigators.

THEORETICAL CONSIDERATIONS

Bottom cavity length

The estimation of the bottom cavity length is based on projectile theory. Figure 1 provides a schematic diagram of the jet flow over an aerator. For a control volume of per unit

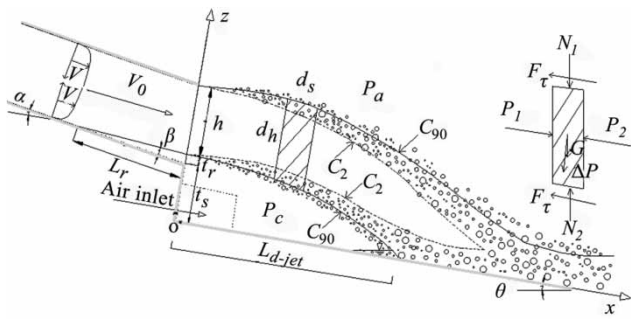

Figure 1 | Sketch of the flow over an aerator.

width (length: ds, thickness: dh): the density of the air–water flow is $\rho_m = (1-C)\rho_w + C\rho_a$, and the weight is $m = \rho_m dV = \rho_m dhds$. The forces acting on the control volume include the following:

Gravity: $G = \rho_m g dhds$

Buoyancy of the air on a nappe: $F_a = \rho_a g dhds$

Vertical pressures: $\frac{dh}{h}\Delta p ds = \frac{dh}{h}(p_a - p_c)ds$

Pressures in the x-direction: $p_1 \approx p_2$

Vertical surface tensions: $N_{1,2} = \frac{\sigma}{R}ds$

Air resistance: $F_\tau = 0.5 c_f \rho_a v^2 ds$

where v is the cross-sectional mean velocity, approximately equal to the mean velocity (v_0) at the pressure-outlet; σ is the coefficient of surface tension ($\sigma = 0.07275\ \mathrm{Nm^{-1}}$); R is the radius of curvature; and c_f is the coefficient of air resistance, $c_f = 0.0125$ (Yang *et al.* 1996).

Among the above-described forces, gravity, buoyant force, pressure, and air drag are the main forces that must be considered, whereas surface tension can be neglected. Then, the expression of the jet trajectory can be written as

$$\begin{cases} \dfrac{dV_x}{dt} = \dfrac{(1-C)(\rho_w-\rho_a)}{\rho_m} g\sin\theta - \dfrac{0.5 c_f \rho_a v_0^3}{\rho_m q} \\ \dfrac{dV_z}{dt} = -\left[\dfrac{(1-C)(\rho_w-\rho_a)}{\rho_m}\cos\theta + P_N\right] g \end{cases} \quad (1)$$

where $P_N = (p_a - p_c)/\rho_w g h$ is the sub-pressure beneath the cavity; p_a and p_c are the pressures close to the free surface and internal cavity, respectively; and ρ_a, ρ_w and ρ_m are the density of the air, water and air–water mixture flow, respectively.

The initial boundary conditions are as follows:

$$\begin{cases} x|_{t=0} = 0,\ V_x|_{t=0} = v_i\cos\phi \\ z|_{t=0} = t_r + t_s,\ V_z|_{t=0} = v_i\sin\phi \end{cases} \quad (2)$$

The expression for calculating the bottom cavity length can be obtained by using Equations (1) and (2) as follows:

$$L_{d-jet} = K_1 T + K_2 T^2 \quad (3)$$

where $K_1 = v_i\cos\phi$ and $K_2 = \frac{1}{2}\left(\frac{(1-C)(\rho_w-\rho_a)}{\rho_m} g\sin\theta - \frac{0.5 c_f \rho_a v_0^3}{\rho_m q}\right)$. The flow jet was assumed to be formed by a solid particle, and its flight time T was defined as

$$T = \frac{v_i\sin\phi}{\left(\frac{(1-C)(\rho_w-\rho_a)}{\rho_m}\cos\theta + P_N\right)g} \cdot \left(1 + \sqrt{1 + 2g(t_r+t_s)\left(\frac{(1-C)(\rho_w-\rho_a)}{\rho_m}\cos\theta + P_N\right)/(v_i\sin\phi)^2}\right)$$

and v_i can be calculated by modifying the mean velocity at the pressure outlet as $v_i = \sqrt{v_0^2 + v'^2}$, where v_0 is the mean velocity. Based on the results of Pope (2000), the fluctuating velocity v' can be calculated as $v' = \frac{v_0}{5\log_{10}(2v_0h_0/\nu) - 2.4}$, where $\nu = 1.01\times10^{-6}\ \mathrm{m^2 s^{-1}}$ is the kinematic viscosity coefficient, C is the mean air concentration, and ϕ is the emergence angle of the jet. According to the present experiments and the results of Wu & Ruan (2008), an improved expression for the emergence angle is given as $\phi = \beta\sqrt{\tanh\left(\frac{t_r}{h_0\beta}e^{\frac{2.7725}{Fr-1}}\right)} + (\theta-\alpha) - \arctan\frac{v'}{v_0}$; θ is the angle with respect to the horizontal; g is the acceleration of gravity.

The trajectory equations of the lower nappe can be expressed as

$$\begin{cases} x = (v_i\cos\phi)t + \dfrac{1}{2}\left(\dfrac{(1-C)(\rho_w-\rho_a)}{\rho_m} g\sin\theta - \dfrac{0.5 c_f \rho_a v_0^3}{\rho_m q}\right)t^2 \\ z = (v_i\sin\phi)t - \dfrac{1}{2}\left(\dfrac{(1-C)(\rho_w-\rho_a)}{\rho_m}\cos\theta + P_N\right)gt^2 + (t_r+t_s) \end{cases} \quad (4)$$

The overall factors that affect the bottom cavity length, including the aeration, the cavity pressure, the emergence angle and the aerodynamic drag, were considered in Equations (3) and (4).

Lateral cavity length

As is generally known, hydrodynamic pressure is always generated when water flows in a pressure-tunnel. The cross-sectional distribution of hydrodynamic pressure is that it is higher near the center and lower near the circumference (Ai & Shen 1995). The water cannot diffuse because of the restriction of the surrounding wall. When the water flow arrives at the sudden fall-expansion aerator, the pressure around the water surface immediately changes to atmospheric pressure whereas the hydrodynamic pressure inside the water remains high. The internal high pressure must inevitably spread to the surrounding water-free surfaces, resulting in the water spreading. Additionally, the high-speed water within the intense turbulence and the Reynolds stress can affect the transverse diffusion flow too (Ghasemi *et al.* 2015). The two factors mentioned can be integrated and expressed as a transverse force F that results in the formation of the side cavity.

Figure 2 is the schematic diagram of the lateral aeration flow. The weight is $m = \rho_m dV = \rho_m dB ds$ for a control volume of unit height (width dB and length ds). The forces acting on the control volume include the following:

Side surface tensions: $N_1 = \dfrac{\sigma}{R} ds$

Air resistance: $F_\tau = 0.5 c_f \rho_a v^2 ds$

Pressures in the x-direction: $p_1 \approx p_2$

Transverse force: F

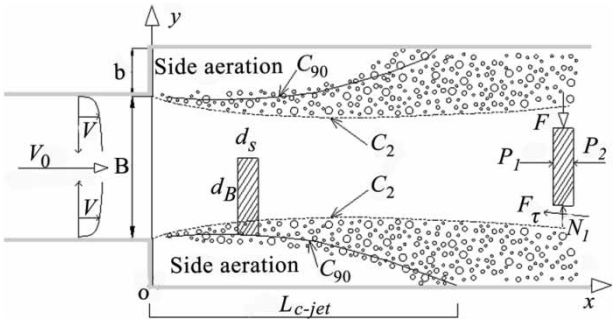

Figure 2 | Flow pattern of the aerator with lateral enlargement.

The definitions of the symbols are the same as those noted above.

Under the conditions in this test, the air resistance of the lateral nappe is approximately 0.002418–0.0054 N, which is a microscopic force that can be ignored. Analogous to the aforementioned analysis of the lower nappe, the trajectory of the lateral nappe (x–y coordinates) can be written as

$$\begin{cases} x = v_0 t \\ y = -0.5 a_y t^2 + u_y t + b \end{cases} \tag{5}$$

where a_y is the acceleration along the transverse direction, u_y is the lateral diffusion velocity, and b represents the width of the lateral expansion.

Then, the trajectory of the lateral nappe can be expressed in the following form:

$$y = -\frac{a_y}{2v_0^2} x^2 + \frac{u_y}{v_0} x + b \tag{6}$$

The lateral cavity length can be expressed as

$$L_{c-jet} = v_0 T = v_0 \frac{u_y + \sqrt{u_y^2 + 2a_y b}}{a_y} \tag{7}$$

Equation (7) is derived from Equation (5), including two main parameters (u_y and a_y), which are crucial to determining the cavity length. A dimensional analysis was performed to determine those two parameters in this research.

Based on the present experiments and the previous studies, the lateral cavity length is considerably influenced by the following factors: (1) the bottom slopes upstream (α) and downstream (θ) of the aerator, the lateral width b and the drop height t_s; (2) the flow velocity v_0 and the depth h; (3) the pressure in the lateral cavity p_c' and the gravitational acceleration g; and (4) the density of air–water ρ_m, the dynamic viscosity coefficient μ, and the surface tension σ. In this study, the Reynolds number is approximately $(0.89–1.24) \times 10^6$, which is large enough to ignore the viscous force. There is no negative pressure in the lateral cavity because of good ventilation conditions. The surface tension has less effect on a high velocity flow. Then, the dimensional analysis of the cavity length yields

$$L_{c-jet} = f(h, g, \rho_m, v_0, b, t_s, \alpha, \theta) \tag{8}$$

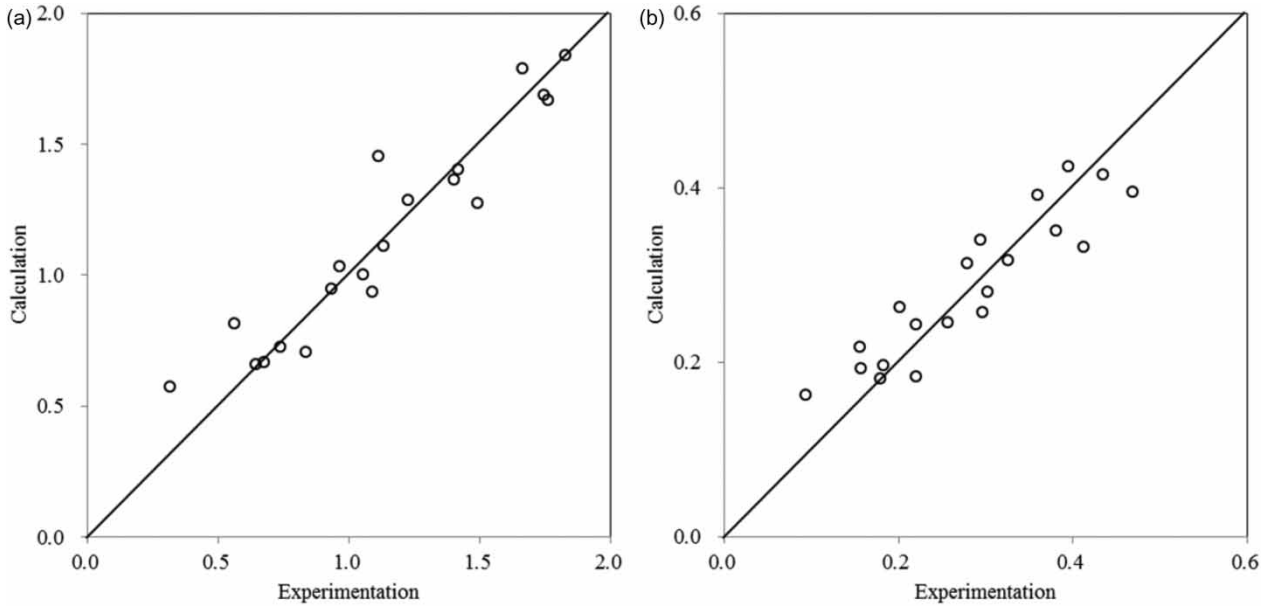

Figure 3 | Comparison of the experimental data and calculation results: (a) a_y/g; (b) $u_y/(gh)^{0.5}$.

The independent dimensions h, ρ_m and g, which include [L], [T] and [M], were employed in the present dimensional analysis, namely, $[h] = [L^1T^0M^0]$, $[g] = [L^1T^{-2}M^0]$ and $[\rho_m] = [L^{-3}T^0M^1]$. The remaining variables can be represented by the three basic dimensions as follows: $\pi = \frac{L_{c-jet}}{h^x g^y \rho_m^z}$; $\pi_1 = \frac{v}{h^{x_1} g^{y_1} \rho_m^{z_1}}$; $\pi_2 = \frac{b}{h^{x_2} g^{y_2} \rho_m^{z_2}}$; $\pi_3 = \frac{h}{h^{x_5} g^{y_5} \rho_m^{z_5}}$; $\pi_4 = \alpha$; $\pi_5 = \theta$; and $\pi_6 = \beta$.

According to the principle of dimensional harmony, the exponents are determined as follows: $x = 1$, $y = 0$ and $z = 0$ for $\pi = \frac{L_{c-jet}}{h^x g^y \rho_m^z}$, namely, $\pi = \frac{L_{c-jet}}{h}$. Similarly, $\pi_1 = \frac{v_0}{\sqrt{gh}} = Fr$, $\pi_2 = \frac{b}{h}$ and $\pi_3 = \frac{t_s}{h}$.

Then, the expression for calculating the lateral cavity length is as follows:

$$\frac{L_{c-jet}}{h} = F\left(\frac{v_0}{\sqrt{gh}}, \frac{b}{h}, \frac{t_s}{h}, \alpha, \theta\right) \quad (9)$$

A series of experiments were conducted to determine the parameters in Equation (9). The results indicate a positive correlation between the lateral cavity length and the width of the lateral aerator (b), the Froude number (F_r), the bottom slopes (θ) and the height of the aerator (t_s). Therefore, those parameters are summarized in the dimensionless parameter X^*, which can be written as follows:

$$X^* = \left(\frac{v_0}{\sqrt{gh}}\right)^2 \left(\frac{b}{B+2b}\right)^{0.15} \left(\frac{t_s}{h}\right)^{0.1} (\cos\theta)^{-2} \quad (10)$$

The relationships of the dimensionless acceleration a_y/g and the dimensionless velocity $u_y/(gh)^{0.5}$ with X^* are

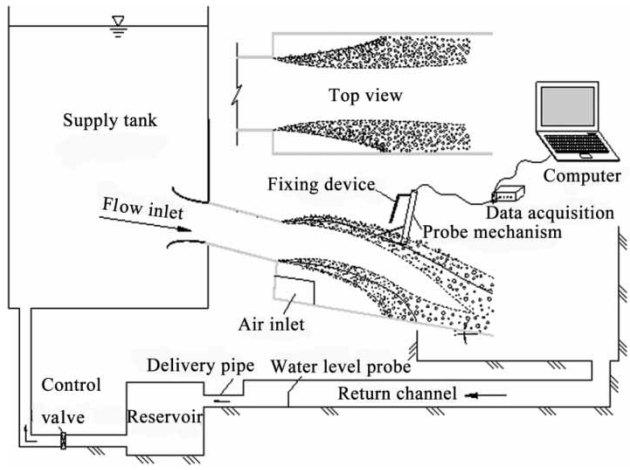

Figure 4 | Schematic of the experimental test equipment.

Table 1 | Experimental flow conditions

Series	(t_s, b) /(m,m)	θ	F_r	R_e ($\times 10^6$)
1	(0.025,0.000)	10%	4.95–7.42	0.89–1.34
2	(0.045,0.000)	10%	4.95–7.42	0.89–1.34
3	(0.065,0.000)	10%	4.95–7.42	0.89–1.34
4	(0.000,0.025)	10%	4.95–7.42	0.89–1.34
5	(0.000,0.045)	10%	4.95–7.42	0.89–1.34
6	(0.000,0.065)	10%	4.95–7.42	0.89–1.34
7	(0.025,0.025)	10%	4.95–7.42	0.89–1.34
8	(0.045,0.045)	10%	4.95–7.42	0.89–1.34
9	(0.065,0.065)	10%	4.95–7.42	0.89–1.34
10	(0.045,0.045)	0%	4.95–7.42	0.89–1.34
11	(0.000,0.045)	0%	4.95–7.42	0.89–1.34
12	(0.045,0.000)	0%	4.95–7.42	0.89–1.34
13	(0.045,0.045)	25%	4.95–7.42	0.89–1.34
14	(0.000,0.045)	25%	4.95–7.42	0.89–1.34
15	(0.045,0.000)	25%	4.95–7.42	0.89–1.34

described as follows:

$$\begin{cases} \dfrac{a_y}{g} = 0.027(X^*)^{1.15} \\ \dfrac{u_y}{(gh)^{0.5}} = 0.013(X^*)^{0.95} \end{cases} \tag{11}$$

Equation (11) was also tested against the experimental data, and the result is shown in Figure 3. It can be seen that the calculation results agree well with the experimental data.

VERIFICATION OF THE PRESENT METHOD

The present equations of cavity length were validated through comprehensive experimental tests. Figure 4 shows a schematic of the rectangular flume setup. The experimental parameters are summarized in Table 1. The chute size

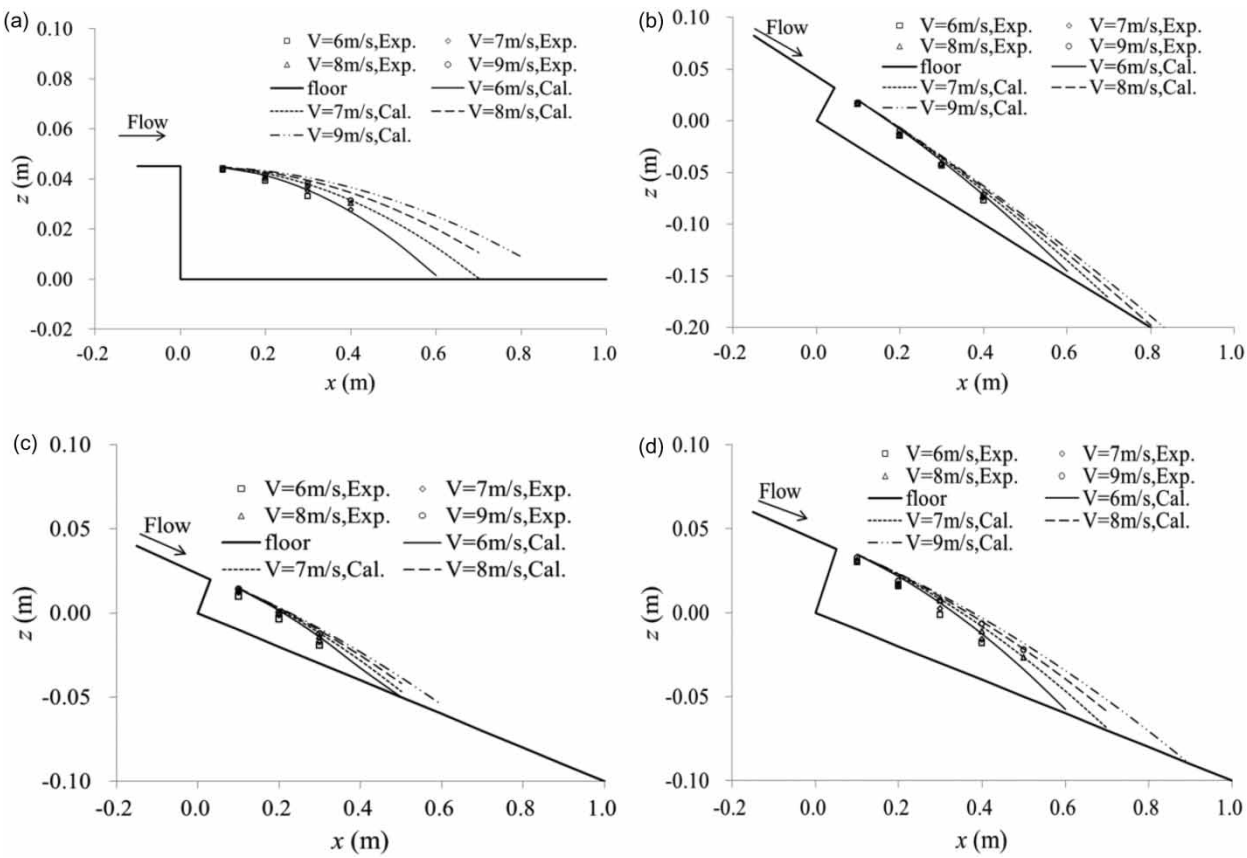

Figure 5 | Comparison of the experimental data with the calculated values of the trajectory of the bottom cavity: (a) (t_s, b) = (4.5 cm, 4.5 cm), θ = 0%; (b) (t_s, b) = (2.5 cm, 2.5 cm), θ = 25%; (c) (t_s, b) = (2.5 cm, 2.5 cm), θ = 10%; (d) (t_s, b) = (4.5 cm, 4.5 cm), θ = 10%.

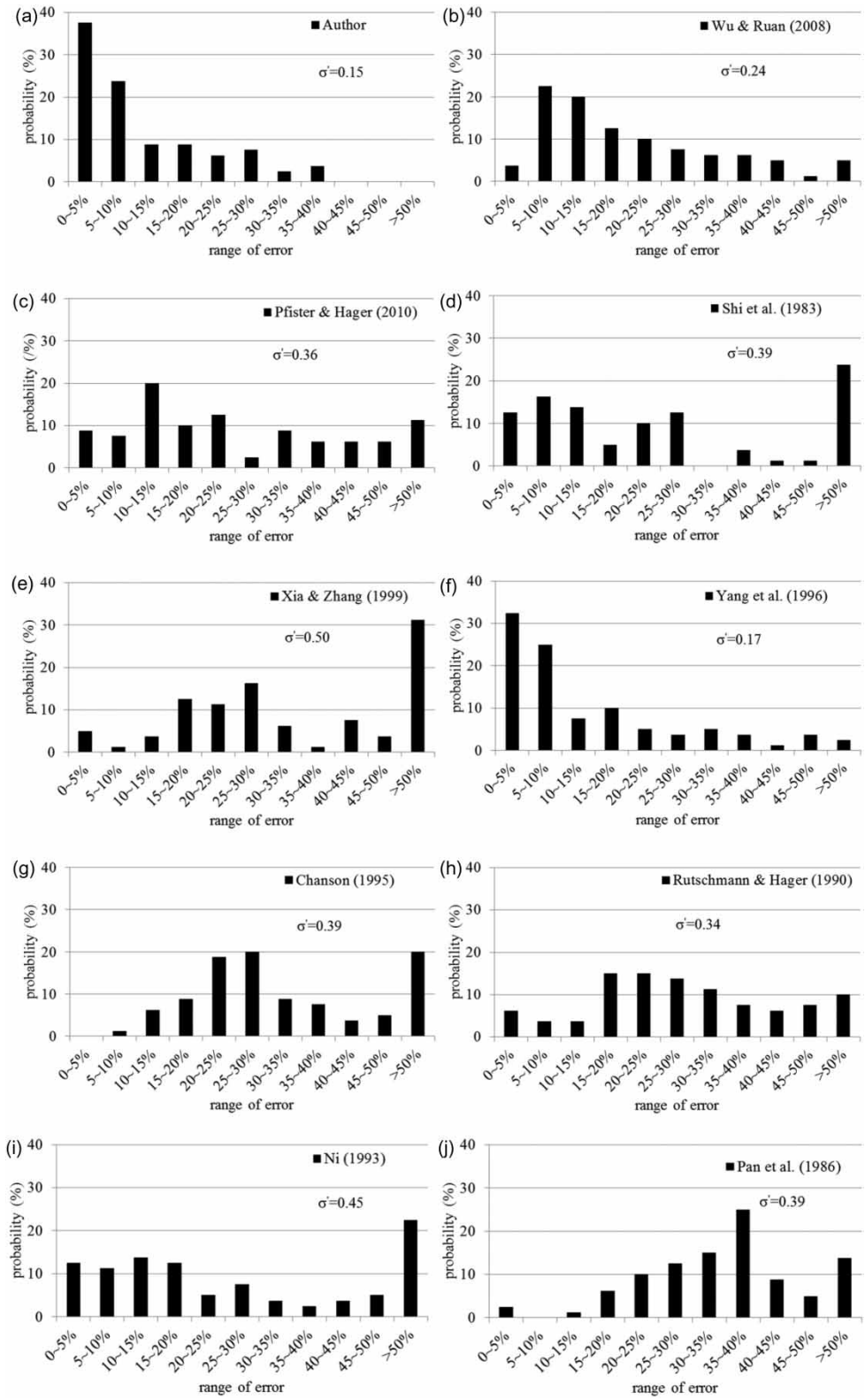

Figure 6 | The relative error of various methods.

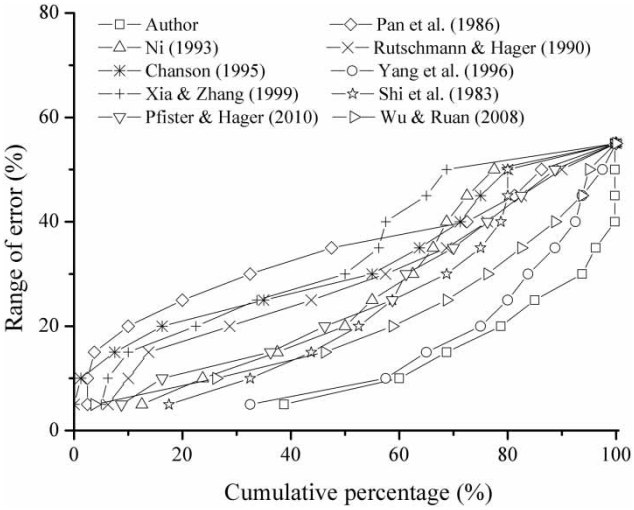

Figure 7 | The cumulative error of various methods.

downstream of the aerator is 3.5 m × 0.3 m × 0.5 m (length × width × height).

The trajectories of the lower nappe (Equation (4)) are used to fit the experimental data. The result proves the goodness of fit illustrated in Figure 5. The geometric shape of the bottom cavity presents a parabolic distribution. The results also indicated that the present expression has an error of 12%, reflecting the fluctuation of bottom cavity length, caused by the air–water mixture flow.

Equation (3) also fits 80 data from 12 aerators of eight hydropower projects, including Foz do Areia (Pinto *et al.* 1982), Dongjiang, Lubuge, Fengjiashan, Nuozhadu, Shitouhe, Wujiangdu and Xizhijiang (Ni 1993). Here, the relative error (Δ) between the calculated results ($L_{\text{calculated}}$) and the measured values (L_{measured}), and the root mean square error (σ') were adopted (see Equation (12)) to verify the precision of different formulas:

$$\begin{cases} \Delta = (L_{\text{calculated}} - L_{\text{measured}})/L_{\text{measured}} \\ \sigma' = \left(\sum_{i=1}^{N} [(L_{\text{calculated}} - L_{\text{measured}})/L_{\text{measured}}]^2 / N \right)^{0.5} \end{cases} \quad (12)$$

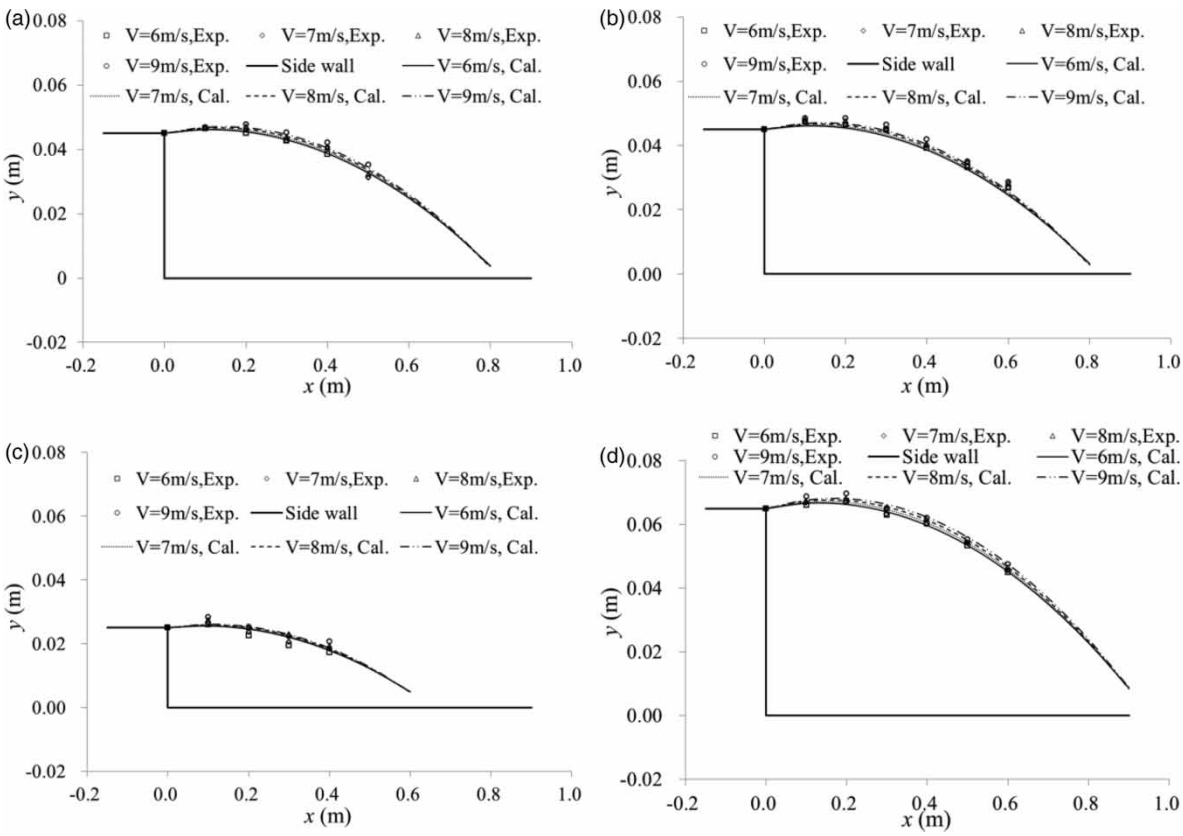

Figure 8 | Comparison of the experimental data with the calculated values of trajectory of the lateral cavity: (a) (t_s, b) = (4.5 cm, 4.5 cm), θ = 0%; (b) (t_s, b) = (4.5 cm, 4.5 cm), θ = 25%; (c) (t_s, b) = (2.5 cm, 2.5 cm), θ = 10%; (d) (t_s, b) = (6.5 cm, 6.5 cm), θ = 10%.

The root mean square error, the relative error and cumulative error of the formulas are shown in Figures 6 and 7, respectively. Generally, the results demonstrate that the present method has a relative higher accuracy than other methods. The reason may be that this research accounts for more factors which affect the cavity length. It is noted that the accuracy of the method of Yang *et al.* (1996) is slightly lower than the present method. The reason may be that it does not account for the influence of aeration on the cavity.

Equation (7) was also tested against the experimental tests (Figure 8), indicating a good agreement between the predictions and observations. The result shows that the morphology of the lateral cavity obeys a quadratic parabolic curve, caused by the gradually decay of both the internal pressure and the Reynolds stress, which is consistent with the theoretical analysis.

To validate the precision of the equation of lateral cavity length, the data of these experiments and Wang *et al.* (2013) and Liu *et al.* (2015) are plotted in Figure 9. It can be seen that the present calculation results are consistent with the test data. Again, it is proved that Equation (7) can be adopted for calculating the lateral cavity length. Additionally, some discrete data still exist, caused by errors of the measuring instruments or the different definitions of the cavity length.

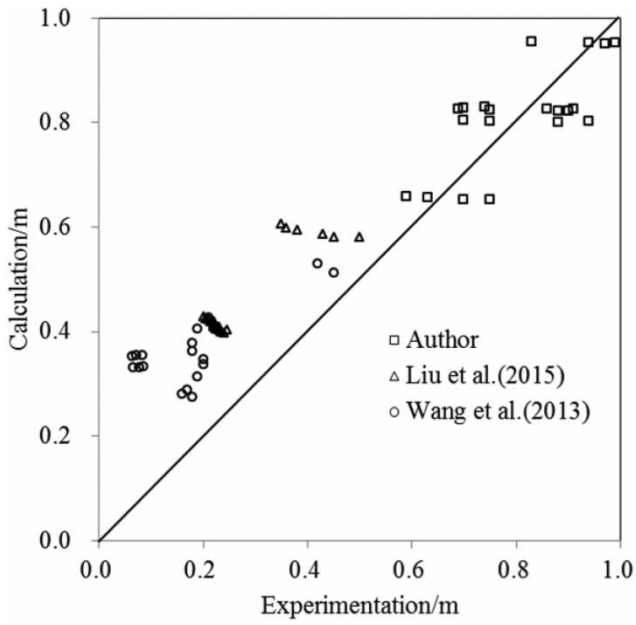

Figure 9 | Comparison of the calculated and experimental data.

CONCLUSIONS

In this study, the factors affecting the cavity length downstream of a sudden fall-expansion aerator are investigated for various aerator sizes and approach-flow velocities. The following conclusions can be drawn:

(1) An improved expression for calculating the geometrical morphology and the length of bottom and lateral cavities is established. When compared with other empirical equations, the proposed equation has a higher precision.
(2) Preliminary analysis of the formation mechanism of the lateral cavity revealed that the lateral cavity is mainly caused by dynamic pressure and transverse turbulent stress. The morphology of the lateral cavity exhibited a quadratic parabolic distribution, which is similar to the curve of the bottom cavity.

FUNDING

This work was partly supported by China Postdoctoral Science Foundation (grant 2016M602716), the CAS 'Light of West China' Program (grant Y6R2220220), the National Science Fund for Distinguished Young Scholars (grant 51625901), the Natural Science Foundation of China (grant 51579165) and the Young Scientists Research Fund of the Institute of Mountain Hazards and Environment CAS (grant Y6K2080080).

REFERENCES

Aghebatie, B. & Hosseini, K. 2016 Analyzing the turbulent flow on steep open channels. *Water Science and Technology: Water Supply* **16** (5), 1207–1213. doi: 10.2166/ws.2016.043.

Ai, C. & Shen, Z. H. 1995 Study of pressure distribution in jets under ambient pressure condition. *Petroleum Drilling Techniques* **23**, 6–7, 26 (in Chinese).

Chanson, M. H. 1995 Predicting the filling of ventilated cavities behind spillway aerators. *Journal of Hydraulic Research* **33** (3), 361–372. doi: 10.1080/00221689509498577.

Ghasemi, A., Roussinova, V., Balachandar, R. & Barron, R. M. 2015 Reynolds number effects in the near-field of a turbulent square jet. *Experimental Thermal and Fluid Science* **61**, 249–258. doi: 10.1016/j.expthermflusci.2014.10.025.

Hager, W. H. & Boes, R. M. 2014 Hydraulic structures: a positive outlook into the future. *Journal of Hydraulic Research* **52** (3), 299–310. doi: 10.1080/00221686.2014.923050.

Liu, C., Zhang, G. K. & Li, N. W. 2008 The effect of base aerator on the length of lateral cavity. *Journal of Sichuan University (Engineering Science Edition)* **40**, 1–4 (in Chinese).

Liu, C., Li, L. G., Zhuang, W. H., Li, N. W. & Liu, H. F. 2015 Research on cavity length of aerator with sudden lateral enlargement and vertical drop in free flow chute. *Journal of Sichuan University (Engineering Science Edition)* **47**, 1–5 (in Chinese).

Mohaghegh, A. & Wu, J. H. 2009 Effects of hydraulic and geometric parameters on downstream cavity length of discharge tunnel service gate. *Journal of Hydrodynamics, Ser. B* **21** (6), 774–778. doi: 10.1016/S1001-6058(08)60212-7.

Ni, H. G. 1993 *Nuclei-Cavitation-Cavitation Erosion.* Chengdu Science and Technology University Press, Chengdu, China (in Chinese).

Nie, M. X., Wang, X. S. & Wu, G. H. 2003 Effect of lateral deflector on outlet cavity lengths. *Journal of Hydraulic Engineering* **129** (7), 536–540. doi: 10.1061/(ASCE)0733-9429(2003)129:7(536).

Pan, S. B. & Shao, Y. Y. 1986 Hydraulic estimation of a U-shape abrupt off-set aeration device. *Journal of Hydraulic Engineering* **8**, 12–20 (in Chinese).

Pfister, M. & Hager, W. H. 2010 Chute aerators. I: air transport characteristics. *Journal of Hydraulic Engineering* **136** (6), 352–359. doi: 10.1061/(ASCE)HY.1943-7900.0000189.

Pfister, M., Lucas, J. & Hager, W. H. 2011 Chute aerators: pre-aerated approach flow. *Journal of Hydraulic Engineering* **137** (11), 1452–1461. doi: 10.1061/(ASCE)HY.1943-7900.0000417.

Pinto, N. L. de S., Neidert, S. H. & Ota, J. J. 1982 Aeration at high velocity flows: part one. *International Water Power and Dam Construction* **34**, 34–38.

Pope, S. B. 2000 *Turbulent Flows.* Cambridge University Press, Cambridge, UK, pp. 264–281.

Rutschmann, P. & Hager, W. H. 1990 Design and performance of spillway chute aerators. *International Water Power and Dam Construction* **42**, 36–42.

Shi, Q. S., Pan, S. B., Shao, Y. Y. & Yuan, X. Y. 1983 Experimental investigation of flow aeration to prevent cavitation erosion by a deflector. *Journal of Hydraulic Engineering* **14**, 1–13 (in Chinese).

Wang, J. Y., Liu, Z. P., Zhang, J. M. & Jiao, X. Y. 2013 Study on cavity length of sudden lateral enlargement and bottom drop aerator device. *South-To-North Water Transfers and Water Science & Technology* **11**, 28–30 (in Chinese).

Wu, J. & Ma, F. 2013 Cavity flow regime for spillway aerators. *Science China Technological Sciences* **56** (4), 818–823. doi: 10.1007/s11431-013-5145-1.

Wu, J. H. & Ruan, S. P. 2008 Cavity length below chute aerators. *Science in China Series E: Technological Sciences* **51** (2), 170–178. doi: 10.1007/s11431-008-0009-9.

Wu, J. H., Ma, F. & Dai, H. C. 2011 Influence of filling water on air concentration. *Journal of Hydrodynamics, Ser. B* **23** (5), 601–606. doi: 10.1016/S1001-6058(10)60155-2.

Xia, Y. C. & Zhang, L. M. 1999 *Prototype Observation and Model Test for Engineering Hydraulic.* Electric Power Press, Beijing, China (in Chinese).

Yang, Y. S., Chen, C. Z. & Yu, Q. Y. 1996 A mathematical model for self-aeration capacity of free jet on the aerator. *Journal of Hydraulic Engineering* **27**, 13–21 (in Chinese).

Yue, C., Niu, Z. P. & Li, J. 2009 Calculation of the lateral cavity length. *Science Technology and Engineering* **9**, 1443–1445 (in Chinese).

Zhang, J. M., Chen, J. G., Xu, W. L., Wang, Y. R. & Li, G. J. 2011 Three-dimensional numerical simulation of aerated flows downstream sudden fall aerator expansion in a tunnel. *Journal of Hydrodynamics, Ser. B* **23** (1), 71–80. doi: 10.1016/S1001-6058(10)60090-X.

First received 1 August 2017; accepted in revised form 22 January 2018. Available online 8 February 2018